Supplementary information

Carbon-Modified TiO_2 Catalysts for Oxidative Upcycling of Waste Polyethylene to Dicarboxylic Acids

Yi Hao,†[a] Kaili Wang,†[a] Rongrong Jia,[b] Ping Cheng,[c] Liyi Shi,[a] Xiang Wang [d] and Lei Huang *[a]

[a] Research Center of Nano Science and Technology, College of Sciences, Shanghai University, Shanghai 200444, P. R. China

[b] Department of Physics, College of Sciences, Shanghai University, Shanghai 200444, P. R. China

[c] School of Environmental and Chemical Engineering, Shanghai University, Shanghai 200444, China

[d] State Key Laboratory of Fine Chemicals, School of Chemical Engineering, Dalian University of Technology, Dalian, 116024, China

†These authors contributed equally to this manuscript.

*Corresponding Author.

E-mail: leihuang@shu.edu.cn (L. Huang).

This supplementary data includes:

1. Experimental section

2. Figures S1 to S11

3. Tables S1 to S8

1. Experimental section

1.1. Materials

HDPE powder ($M_w \approx 1.07 \times 10^5$ g/mol) was obtained from Macklin Biochemical Co., Ltd. (Shanghai, China). Titanium dioxide (TiO_2, anatase phase, ≥ 99.8%) and deuterated chloroform ($CDCl_3$, ≥ 99.8 atom% D) were purchased from Aladdin Reagent Co., Ltd. (Shanghai, China). Soluble starch (AR), anhydrous ethanol (≥ 99.7%), and dichloromethane (≥ 99.5%) were supplied by Sinopharm Chemical Reagent Co., Ltd. (Shanghai, China). Deuterated dimethyl sulfoxide (DMSO-d_6, ≥ 99.9 atom% D) was obtained from Sigma-Aldrich (Merck KGaA, Shanghai, China). Post-consumer PE samples, including shopping bags and packaging films, were collected from local supermarkets and convenience stores in the Baoshan District of Shanghai, China.

1.2. Catalyst characterization

The structural and surface properties of the catalysts were comprehensively characterized. Powder X-ray diffraction (XRD) were collected using a Bruker D2 diffractometer with a scan rate of 5° min^{-1} to determine the crystalline phase. Surface composition and chemical states were analyzed by X-ray photoelectron spectroscopy (XPS, Thermo Scientific ESCALAB Xi^+) with Al Kα radiation, and binding energies were calibrated using the C 1s peak at 284.8 eV. Nitrogen adsorption–desorption isotherms were measured on a Micromeritics ASAP 2460 analyzer to determine the Brunauer–Emmett–Teller (BET) surface area, pore volume, and pore size distribution. Elemental composition was quantified by X-ray fluorescence (XRF, Shimadzu XRF-1800). Fourier-transform infrared spectroscopy (FTIR, Thermo Nicolet iS10) was used to identify surface functional groups. The surface acidity was probed by temperature-programmed desorption of ammonia (NH_3-TPD) using a Microtrac BELCAT II chemisorption analyzer. For NH_3-TPD, 50 mg of catalyst was pretreated in helium (40 mL min^{-1}) by heating to 800 °C at 10 °C min^{-1}, saturated with 10% NH_3/He at 50 °C, purged with He for 1 h, and then heated to 800 °C for desorption. Oxygen adsorption behavior was examined via O_2-temperature-programmed desorption (O_2-TPD) using

the same instrument; samples were pretreated in He atmosphere at 600 °C, saturated with 10% O_2/He at 50 °C, purged with He, and then heated to 600 °C. Electron paramagnetic resonance (EPR) spectroscopy was conducted on a Bruker EMX PLUS instrument to evaluate oxygen vacancy concentrations. The carbon content in C/TiO_2 samples was determined using a HIR944 carbon–sulfur analyzer. Raman spectra were recorded on a Horiba LabRAM HR Evolution spectrometer with a 633 nm laser to assess the nature of the surface carbon species.

1.3 Production characterization

After the reaction, the system was cooled to room temperature, and gaseous products were collected using FEP gas sampling bags. The reaction mixture was extracted with a DCM/EtOH solvent under ultrasonication for 5 min. After filtration, the filtrate was concentrated under reduced pressure to obtain the oil product, while the solid residue was dried at 60 °C overnight. The solid conversion rate was calculated as following equation (1):

$$Conversion\ (wt\%) = (1 - \frac{m\ (solid\ residual) - m\ (catalyst)}{m\ (plastic)})\ \times 100\% \quad (1)$$

Elemental analysis (UNICUBE, Elementar) was performed to determine the carbon contents of both the product oil and the original PE feedstock. The carbon molar conversion was calculated using the following equation (2):

$$C_n\ (\%) = \frac{C_{n-oil}}{C_{n-PE}} \times 100\% \quad (2)$$

Where C_n% represents the molar conversion rate of the product oil, $C_{n\text{-}oil}$ denotes the molar amount of carbon in the product oil, and $C_{n\text{-}PE}$ denotes the molar amount of carbon in the feedstock PE.

Due to the incorporation of oxygen into the product molecules, oil yield was also expressed as the mass ratio of product oil to original PE. The calculation is shown in equation (3):

$$Oil/Feedstoke\ （wt\%）= \frac{m_{oil}}{m_{PE}} \quad (3)$$

Where m_{oil} is the mass of the product oil, and m_{PE} is the mass of the feedstock PE.

FTIR spectra were recorded on a Thermo Fisher Nicolet iS10 Fourier transform infrared spectrometer to analyze functional groups of the product oil. Proton nuclear magnetic resonance (^{1}H NMR) spectra were acquired using a Bruker Avance III 500 MHz spectrometer with samples dissolved in DMSO-d_6 at a concentration of approximately 12 mg/mL; the number of scans was 32. For detailed structural analysis, ^{13}C qNMR and distortionless enhancement by polarization transfer (DEPT) spectra were recorded on a Bruker Avance III 600 MHz spectrometer using $CDCl_3$ as solvent with a sample concentration around 200 mg/mL. High-resolution mass spectrometry (HRMS) was performed on a Thermo Orbitrap Fusion Lumos instrument operated in negative-ion electrospray ionization (ESI) mode to determine the molecular composition of the product oil. The dicarboxylic acid products obtained from catalytic oxidation were analyzed by gas chromatography (GC) using a Shimadzu GC-2014C system (Japan) equipped with a flame ionization detector (FID) and an HP-5 capillary column. Prior to GC analysis, the oxidation products were derivatized via esterification. Specifically, 10.00 mL of the product solution was mixed with 5.00 mL of a 50 wt% BF_3–MeOH solution and heated at 70 °C for 1 h. After cooling, the reaction was quenched by adding 2.00 mL of water. The resulting mixture was extracted several times with 5.00 mL portions of *n*-hexane, and the combined organic phases were diluted to a final volume of 10.00 mL. For quantitative analysis, defined amounts of dicarboxylic acid standards (C_4–C_{22}) were dissolved in methanol and diluted to a final volume of 50.00 mL to prepare a series of standard solutions with graded concentrations. These standards were used to construct calibration curves for GC–FID quantification, based on which the carbon yield of the dicarboxylic acid products were determined. The dicarboxylic acid (carbon yield) calculation is shown in following equation (4):

$$Carbon\ yield\ (\%) = \frac{\frac{C * V}{M_{acid}} * n * M_{carbon}}{C_{PE}} \quad (4)$$

Gaseous products were monitored using a time-of-flight mass spectrometer (TOF-MS, Hosin SPIMS-3000), with data collected via the online VOC analysis system. In addition, GC analysis of the gaseous products was carried out using an Agilent 7890B instrument (Agilent Technologies, USA). The system was equipped with a thermal conductivity detector (TCD), and helium (99.99%) was employed as the carrier gas. Gas separation was achieved using a carbon molecular sieve packed column (3 m, 80–100 mesh) for the analysis of permanent gases, including CO_2 and CO. For each analysis, a gas sample volume of 250 μL was injected.

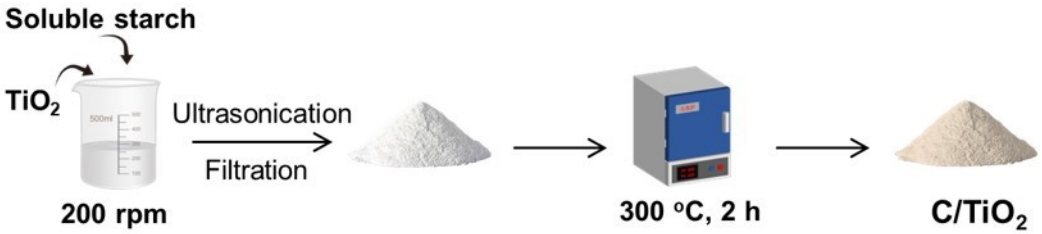

Fig. S1. Schematic illustration of synthesizing C/TiO_2 sample.

Fig. S2. Magnetic stirring reactor for the catalytic oxi-upcycling of PE (KEMN Instruments, CHEMN: NSVP25-P3-T2-SS1-SV-R)

Caution: The oxygen content is controlled within a safe range with the reaction substrate!

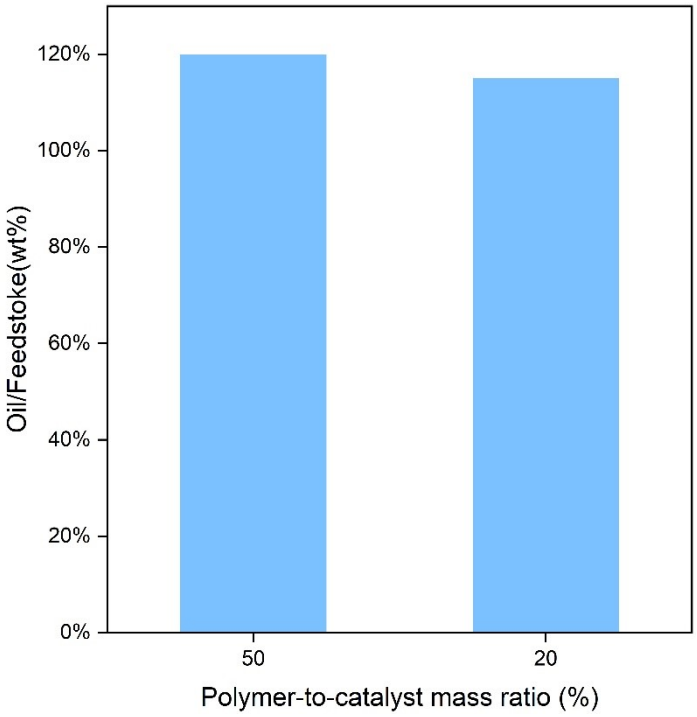

Fig. S3. Effect of catalyst addition on catalytic performance.

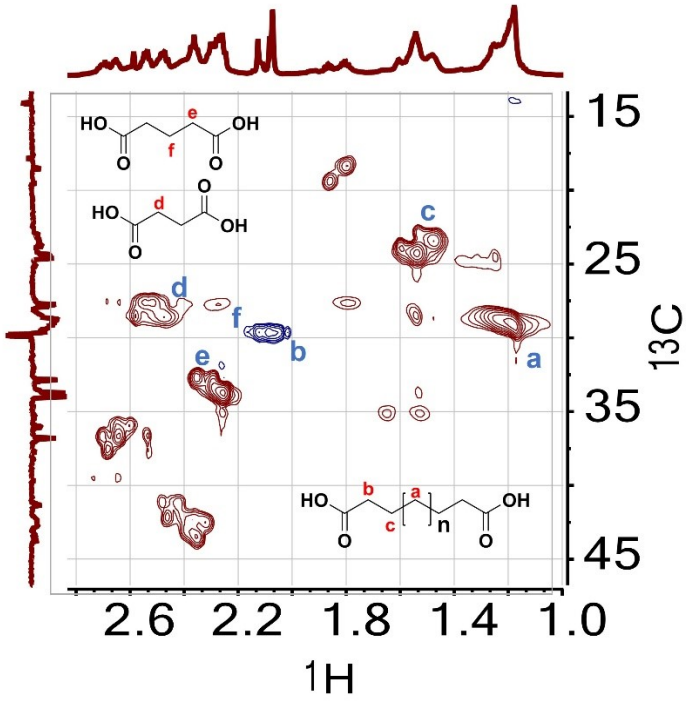

Fig. S4. HSQC of oil product after the oxidation reaction.

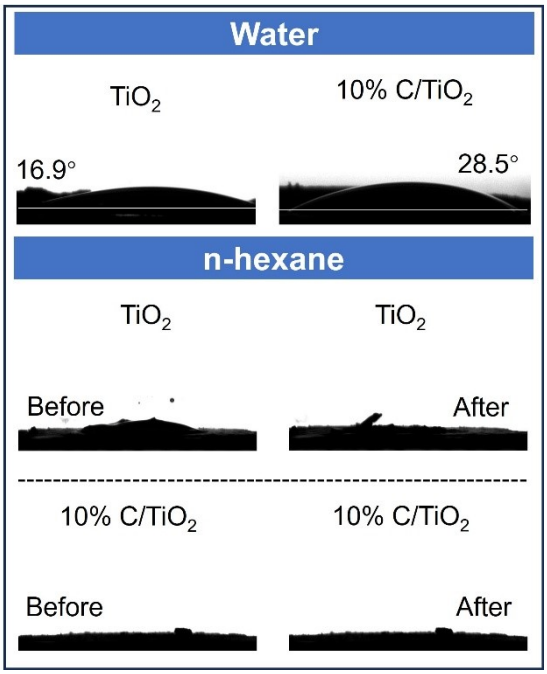

Fig. S5. Water and *n*-hexane contact angles of TiO_2 and C/TiO_2, showing the effect of carbon modification on surface wettability and affinity toward PE

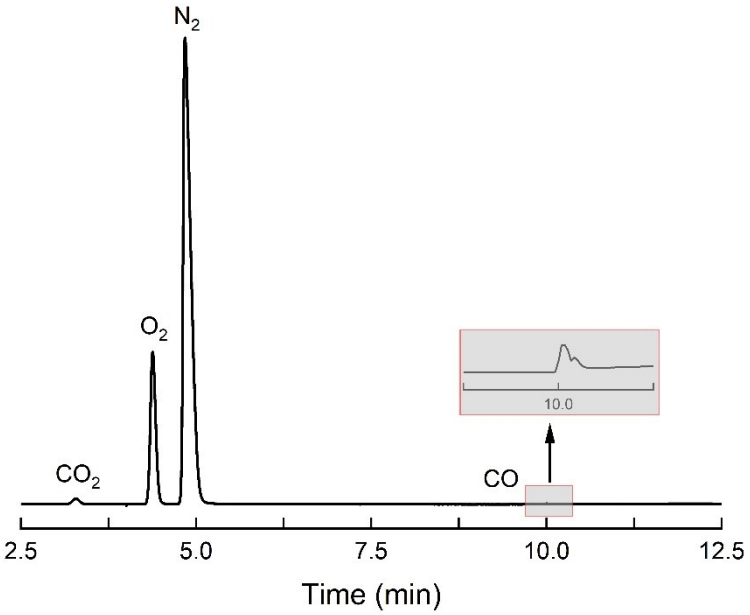

Fig. S6. GC-TCD analysis of the gas products obtained from PE oxidative upcycling using 10% C/TiO_2.

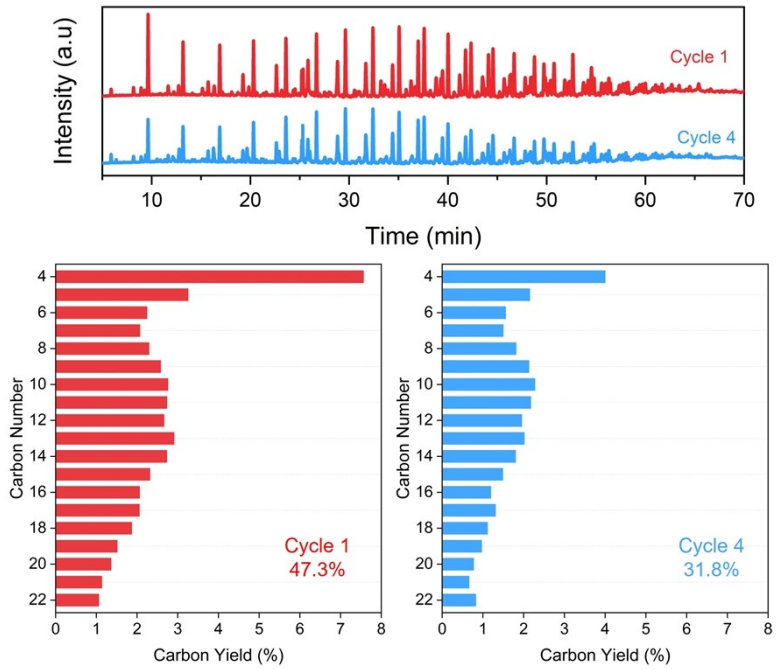

Fig. S7. GC–FID analysis and carbon number distribution of dicarboxylic acid products.

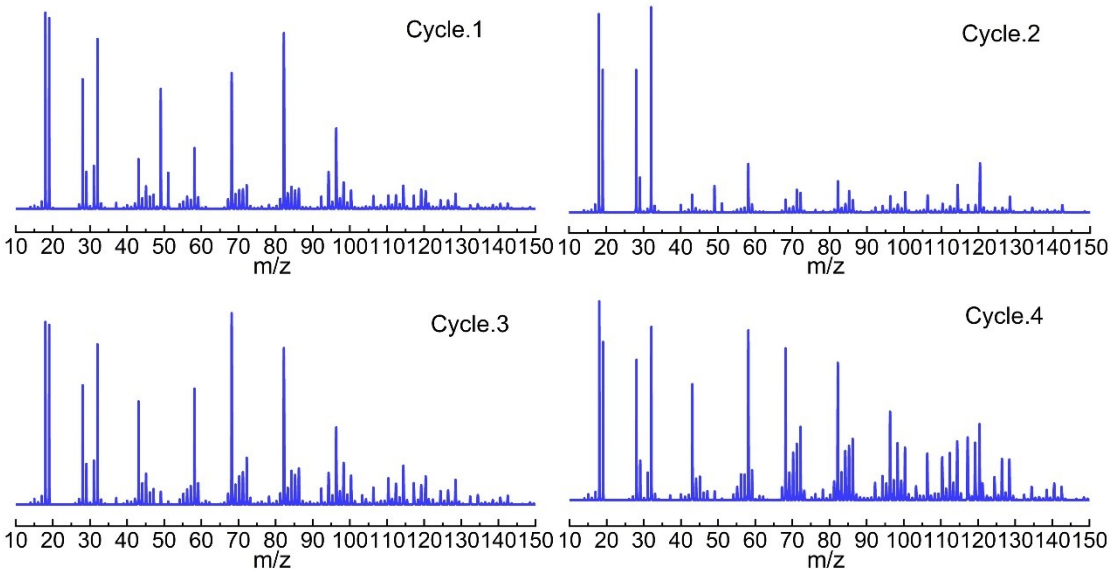

Fig. S8. TOFMS spectra of the gas products of a four-round cycle.

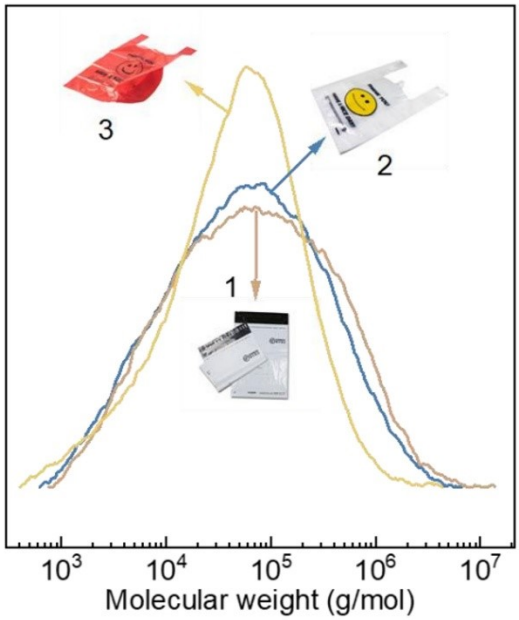

Samples	Mw (g/mol)	Mn (g/mol)	PD
Brown courier bag	1.06×10^5	1.36×10^4	21.54
Plastic shopping bag	1.87×10^5	1.50×10^4	12.33
Red plastic shopping bag	2.40×10^5	1.71×10^4	14.50

Fig. S9. HT-GPC analysis results of actual plastics

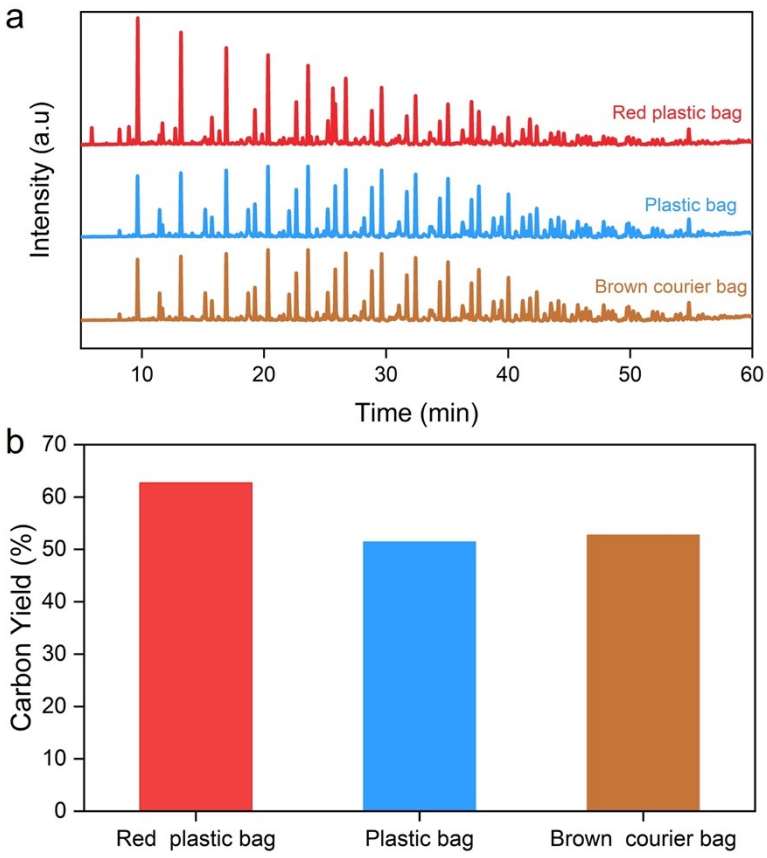

Fig. S10. GC-FID Profiles (a) and dicarboxylic acid yields (b) from catalytic oxidation of different real post-consumer plastics.

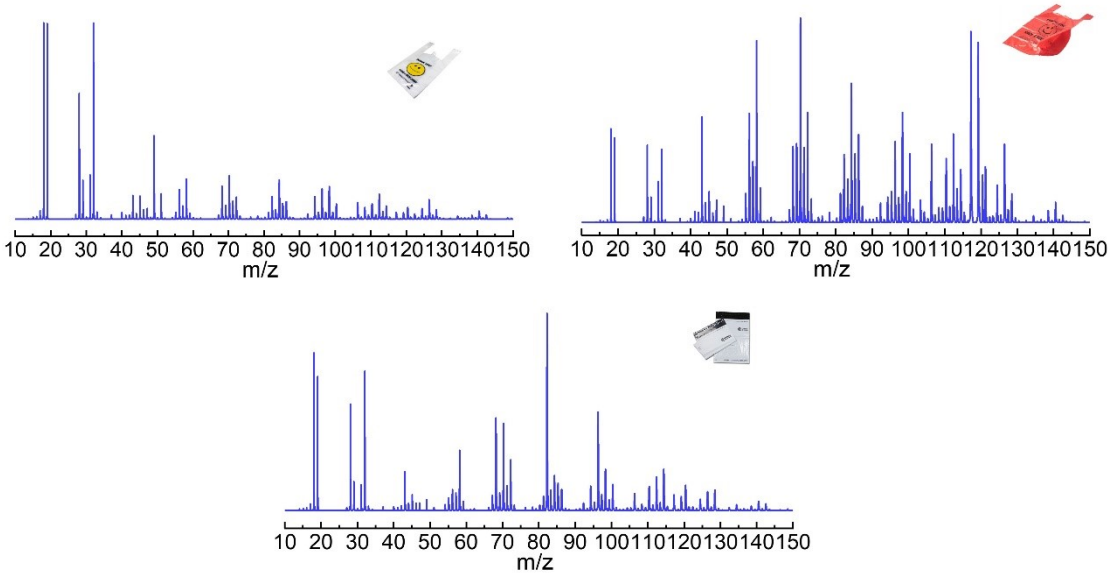

Fig. S11. TOFMS spectra of thermo-catalytic oxi-upcycling of actual PE plastic gas products.

Table S1. Analysis results of nitrogen adsorption and desorption experiments for TiO_2, 10% C/TiO_2 and 40% C/TiO_2.

Samples	**BET** (m^2/g)	**Pore Volume** (cm^3/g)	**Pore Size** (nm)
TiO_2	67	0.36	21.54
10% TiO_2	68	0.31	12.33
40% TiO_2	81	0.31	14.50

Table S2. Analysis of surface C content of 10% C/TiO_2 catalyst.

Samples	C (wt%)
10% C/TiO_2	0.7

Table S3. XRF analysis of O concentration in different catalysts.

Samples	O (%)
TiO_2	40.12
10% C/TiO_2	40.13
40% C/TiO_2	40.11

Table S4. The mass ratio of C and H in the following liquid product samples was detected by elemental analyzer.

Samples	C (wt%)	H (wt%)	C-Mole conversion (%)
HDPE (M_w, 1.07×10^5 g/mol)	86	14	---
Cycle.1, oil	53	7	74
Cycle.2, oil	53	7	62
Cycle.3, oil	51	7	47
Cycle.4, oil	51	7	42

Table S5. The integral ratio of ^{1}H NMR spectra of the cyclic reaction product oil.

Samples	$\frac{H^{-CH_3}}{H^{\beta-carbonyl}}$	$\frac{H^{\beta-carbonyl}}{H^{total}}$
Cycle.1, oil	0.09	0.15
Cycle.2, oil	0.10	0.17
Cycle.3, oil	0.13	0.15
Cycle.4, oil	0.15	0.18

Table S6. The mass ratio of C and H in the following samples was detected by elemental analyzer

Samples	C (wt%)	H (wt%)
Brown courier bag (M_w, 1.06×10^5 g/mol)	79	13
Plastic shopping bag (M_w, 1.87×10^5 g/mol)	86	14
Red plastic shopping bag (M_w, 2.40×10^5 g/mol)	81	13
Brown courier bag (M_w, 1.06×10^5 g/mol), **oil**	56	8
Plastic shopping bag (M_w, 1.87×10^5 g/mol), **oil**	54	8
Red plastic shopping bag (M_w, 2.40×10^5 g/mol), **oil**	52	8

Table S7. The mass ratio of C and H in the following samples was detected by elemental analyzer.

Samples	$\frac{H^{-CH_3}}{H^{\beta-carbonyl}}$	$\frac{H^{\beta-carbonyl}}{H^{total}}$
Brown courier bag (M_w, 1.06×10^5 g/mol), **oil**	0.17	0.18
Plastic shopping bag (M_w, 1.87×10^5 g/mol), **oil**	0.13	0.21
Red plastic shopping bag (M_w, 2.40×10^5 g/mol), **oil**	0.11	0.17

Table S8. Reaction conditions for PE oxidation.

Catalysts	Oxidants	Reaction conditions	Main products	Ref.
Ru/TiO_2 (~ 22300 $/kg)*	1.5 MPa air	160 °C, 24 h	Long-chain dicarboxylic acid	1
Co/MCM-41 (~ 800 $/kg)	1.0 MPa O_2	125°C, 12 h	C_3-C_{20} dicarboxylic acid	2
TS-1 (~ 2800 $/kg)	1.5 MPa air	140-200 °C, 12 h	C_3-C_{20} dicarboxylic acid	3
C/TiO_2 (~ 230 $/kg)	1.5 MPa air	150 °C, 24 h	C_4-C_{22} dicarboxylic acid	**This work**

*The catalyst costs were approximately estimated according to the reported precursor materials and preparation methods described in the corresponding literature.

1. K. Wang, R. Jia, P. Cheng, L. Shi, X. Wang and L. Huang, *Angew. Chem., Int. Ed.*, 2023, **62**, e202301340.
2. Q. Zhang, J. He, X. Wei, C. Shen, P. Ye, W. An, X. Liu, H. Li, S. Xu, Z. Su and Y. Z. Wang, *Angew. Chem., Int. Ed.*, 2024, **63**, e202407510.
3. X. Hou, F. Yuan, X. Liu, K. Wang, Y. Zhu, P. Cheng, R. Jia, L. Shi, L. Huang, *Chem. Eng. J.*, 2025, **504**, 158868.